ELSEVIER

Ceramics International 27 (2001) 755–760

CERAMICS INTERNATIONAL

www.elsevier.com/locate/ceramint

Ultrasonic erosion of whisker-reinforced ceramic composites

Tai-Chiu Lee[a], Deng Jianxin[b,*]

[a]Department of Manufacturing Engineering, The Hong Kong Polytechnic University, Hung Hom, Kowloon, Hong Kong, China
[b]Department of Mechanical Engineering, Shandong University of Technology, Jinan 250061, Shandong province, PR China

Received 19 December 2000; received in revised form 20 January 2001; accepted 1 February 2001

Abstract

Uniaxial hot-pressing of SiC whisker reinforced Al_2O_3 ceramic composites induces an anisotropy in whisker distribution and leads to a composite with anisotropic mechanical properties. In this paper, the effects of whisker orientation on the material removal rates and mechanisms in ultrasonic machining of Al_2O_3/SiC_w ceramic composites are reported. It was found that the material removal rates and machined surface roughness in ultrasonic machining of the composites varied according to the angle θ to the hot pressing direction. The maximum material removal rate and surface roughness were observed for the machining surface perpendicular to the hot-pressing direction ($\theta = 0°$), and the minimum ones were observed for the machining surface parallel to the hot-pressing direction ($\theta = 90°$). This effect was larger for specimens with higher SiC whisker content. Based on the lateral crack fracture analysis in ultrasonic machining of the composites, the mechanisms responsible for the anisotropy in material removal rates caused by whisker orientation were investigated.

Keywords: Ultrasonic machining; Ceramic composite; Whisker orientation

1. Introduction

Monolithic ceramics are characterised by relatively low fracture toughness and probabilistic fracture strength. Considerable improvement in mechanical properties of monolithic ceramics has been achieved by incorporating one or more other components into the monolithic matrix to form a ceramic-matrix composite (CMC) [1,2]. The reinforcing component is in the form of particles, whiskers or fibbers. Whisker reinforced ceramic composites are under intensive development for structural, wear and high temperature applications. They possess the attractive properties common to ceramics such as high melting temperature, high strength at elevated temperatures, low density, and excellent chemical stability, combined with improved fracture toughness, strength and mechanical reliability. The first applications of whisker reinforcement to ceramics were in the alumina and mullite matrix systems [3,4].

Although advances have been made in near-net-shape technology, machining of ceramic composites in the fired condition continues to be the predominant process for close-tolerance structural-ceramic components. Among the various machining processes, grinding with diamond wheel, ultrasonic machining (USM) and electrical discharge machining (EDM) are most widely used [5,6]. The threshold value of ceramic electrical conductivity for EDM is of 100 Ω.cm. As the electrical conductivity of Al_2O_3/SiC_w ceramic composite is insufficient for EDM, ultrasonic machining may be a best solution for complex geometries components made of this composite.

Uniaxial hot-pressing of SiC whisker-reinforced Al_2O_3 ceramic composites induces an anisotropy in whisker orientation normal to the hot-pressing direction and leads to composites with an orientation dependance of the mechanical properties [3,7]. Better values are obtained when the crack plane is perpendicular to the plane of the whiskers. Consequently, the machining of whisker reinforced composite parts such as cutting from hot-pressed cakes has to be adjusted according to whisker orientation [8]. Several studies [8,9] have additionally shown that the friction and wear behaviours and the cutting performances of Al_2O_3/SiC_w ceramic composite were greatly influenced by whisker orientation. The aims of the present investigation are to establish the effect of whisker orientation on material removal rates

* Corresponding author. Tel.: +86-531-2955081, ext. 2047; fax: +86-531-2955999.
E-mail address: dengjx@jn-public.sd.cninfo.net (D. Jianxin).

0272-8842/01/$20.00
PII: S0272-8842(01)00026-8

and mechanisms in ultrasonic machining of Al_2O_3/SiC_w ceramic composites.

2. Materials and experimental procedure

2.1. Material preparation

Monolithic Al_2O_3 (average particle size, 0.5 μm) was used as the base material. 10, 20 and 30 volume fraction of SiC whiskers (diameter 1–2 μm, length 20–80 μm) were added to Al_2O_3 matrix. The dispersion of SiC whiskers was prepared by ultrasonic techniques. The final densification of the compacted mixtures was accomplished by uniaxial hot-pressing at 1840°C with a pressure of 35 MPa in hydrogen atmosphere. Fig. 1 shows schematically the anisotropy of whisker distribution with the direction angle θ of the Al_2O_3/SiC_w composite, where θ represents the direction angle of the surface to XOY surface (normal to the hot pressing direction).

Test pieces of 3×4×36 (mm) prepared from the hot-pressed cakes by cutting and grinding using diamond wheel and were used for the measurement of flexural strength. Flexural strength was evaluated in three-point-bending mode over a 30 mm span, at a crosshead speed of 0.5 mm/min; the single-edge notched beam (SENB) method was used for fracture toughness measurements. The SENB specimens were fractured in four-point-bending mode with outer and inner span dimensions of 24 and 12 mm respectively, and at crosshead speed of 0.1 mm/min. Data on the flexural strength and fracture toughness were gathered on 10 samples for each investigated composition.

2.2. Experimental procedure

The ultrasonic machining test was performed with a J93025 type USM machine tool. The specifications of the machine tool and the test conditions are listed in Table 1. To find the effect of whisker orientation on the material removal rates (MRR) and mechanisms in USM of Al_2O_3/SiC_w composites, five types of test samples with $\theta = 0$, 30, 45, 60, and 90° surface as the machining surface were prepared from the hot pressed cakes. The material removal rate was defined as the ratio of volume loss to machining time. The surface roughness measurements for the machined specimens were carried out on a Talysurf 10 system. The machined surfaces were examined by scanning electron microscopy (SEM).

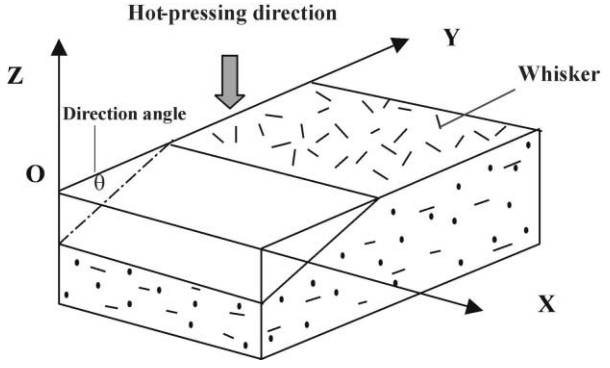

Fig. 1. Schematic of the anisotropy of whisker distribution with direction angle θ in uniaxial hot-pressing SiC whisker reinforced Al_2O_3 ceramic composite.

Table 1
Specifications of the USM machine tool and test conditions

Nominal output power	250 (W)
Frequency	16–25 (kHz)
Amplitude of vibration	5–20 (μm)
Static load	10 (N)
Tool material	Mild steel (Φ5)
Abrasive particle	B_4C (80 grit)

3. Results

3.1. Mechanical properties and characterization of Al_2O_3/SiC_w ceramic composites

Fig. 2 shows the whisker distribution of the Al_2O_3/SiC_w composite along the $\theta = 0$, 45 and 90° surfaces respectively. The fracture toughness and flexural strength of the Al_2O_3/SiC_w composites with different SiC_w content are listed in Table 2, where $\theta = 0°$ represents tensile surface parallel to the whisker plane, and $\theta = 90°$ perpendicular to the whisker plane. It can be observed that whisker orientation leads to anisotropy in both fracture and flexural strength. The fracture toughness rises from 5.5 $MPa.m^{1/2}$ at $\theta = 0°$ to 8.6 $MPa.m^{1/2}$ at $\theta = 90°$ for specimen C, representing a maximum fracture toughness increase of 156% (see Table 2).

3.2. Material removal rates

In ultrasonic machining, the material removal rate of Al_2O_3/SiC_w composites with different SiC_w contents (specimen A, B and C) is a function of θ, as shown in Fig. 3. Whisker orientation exerted an important effect on the MRR. As θ varied from 0 to 90°, a decrease in MRR was observed. The $\theta = 90°$ surface had the smallest MRR, and the $\theta = 0°$ surface had the highest one. This effect was longer for the specimen with higher SiC whisker content. The MRR decreases from 0.43 mm^3/min at $\theta = 0°$ to 0.19 mm^3/min at $\theta = 90°$ for specimen C, representing a maximum MRR decrease of 165% (see Table 3).

3.3. Surface roughness

Fig. 4 shows the effect of whisker orientation on the surface roughness in ultrasonic machining of $Al_2O_3/$

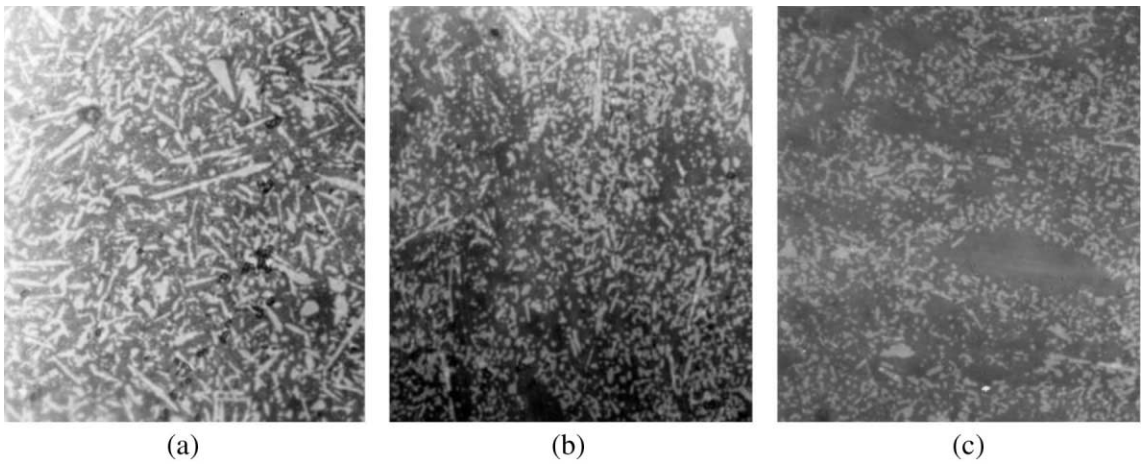

Fig. 2. Whisker distribution of Al_2O_3/SiC_w composite in different surfaces, (a) $\theta=0^\circ$ surface, (b) $\theta=45^\circ$ surface and (c) $\theta=90^\circ$ surface.

Table 2
Anisotropy of fracture toughness and flexural strength of Al_2O_3/SiC_w composites with different SiC whisker content

	SiC (vol.%)	σ_f (MPa) $\theta=0^\circ$	σ_f (MPa) $\theta=90^\circ$	$K_{IC}{}^a$ (MPa.m$^{1/2}$) $\theta=0^\circ$	$K_{IC}{}^b$ (MPa.m$^{1/2}$) $\theta=90^\circ$	$K_{IC}{}^b/K_{IC}{}^a$
A	10	513±23	650±38	4.6±0.2	6.3±0.7	1.37
B	20	556±46	730±55	5.2±0.4	7.6±0.6	1.46
C	30	618±56	767±72	5.5±0.5	8.6±0.8	1.56

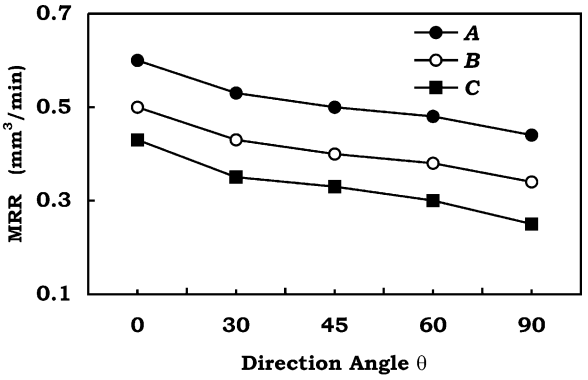

Fig. 3. Material removal rates vs. direction angle θ in ultrasonic machining of Al_2O_3/SiC_w composites with different SiC whisker contents.

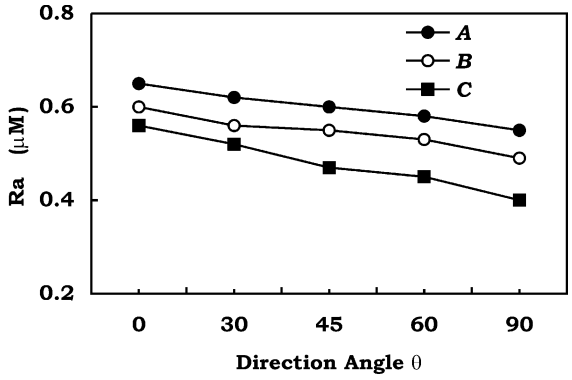

Fig. 4. Surface roughness vs. direction angle θ in ultrasonic machining of Al_2O_3/SiC_w composites with different SiC whisker contents.

Table 3
Anisotropy of MRR of Al_2O_3/SiC_w composites with different SiC whisker content in USM

	MRR ($\theta=0^\circ$) mm^3/min	MRR ($\theta=90^\circ$) mm^3/min	MRR ($\theta=0^\circ$)/MRR ($\theta=90^\circ$)
A	0.60	0.44	1.36
B	0.50	0.34	1.47
C	0.43	0.26	1.65

SiC_w composites with different whisker contents. The effect of whisker orientation on the surface roughness had a similar note than for MRR. The $\theta=90^\circ$ surface exhibited the lowest surface roughness for each specimen. The specimen with higher SiC whisker content exhibited the lower surface roughness among the three specimens tested.

4. Discussion

In Al_2O_3/SiC_w ceramic composites, bridging, whisker pullout and crack deflection are all reported as toughening mechanisms[2]. For a crack plane parallel to the whisker plane (in the case of $\theta=0^\circ$), bridging, whisker pullout and crack deflection is less significant than for a crack plane perpendicular to the whisker plane (in the case of $\theta=90^\circ$). In other words, the crack path approaches the

direction with lower resistance to crack propagation. Thus, the magnitude of fracture toughness increase is controlled by the angle of whisker orientation relative to the hot-pressing direction (see Table 2).

In the USM of ceramics, the abrasive particles in slurry with water are under a tool, which is excited by an ultrasonic frequency with small amplitude, and the material is removed by direct impact of the abrasive particles on the ceramic surface. The material removal by particle impact is thought to occur primarily by surface chipping when lateral cracks curve up and intersect the surface. The most important parameters that control the material removal are identified by indentation fracture mechanics. Fig. 5 illustrates schematically the material removal characteristics by impact-particle. The general equation for material removal in brittle materials, especially in ceramics, by impacting particles is

$$V = \sum N\pi C_L^2 h \tag{1}$$

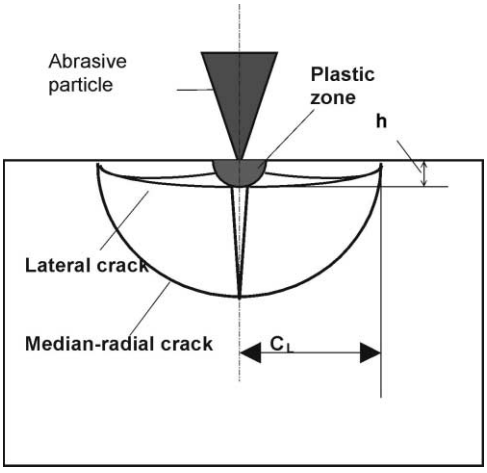

Fig. 5. Schematic illustration of material removal characteristics by impact-particle.

where V is the volume loss, C_L the lateral crack length, h the mean depth, ΣN the total number of impact particles per unit true particle volume. The lateral crack length and the mean depth are given by [10–12]

$$C_L \propto \left[(E/H_V)^{3/4} K_{IC}^{-1} H_V^{-1/4}\right]^{1/2} P^{5/8} \tag{2}$$

$$h \propto (E/H_V)^{1/2} (P/H_V)^{1/2} \tag{3}$$

where E and H_v are Young's modulus and Vickers hardness of the material, and P is the mean vertical impact force acting from one particle to material during machining. Substituting Eqs. (2) and (3) into Eq. (1), the volume removed becomes

$$V = K \sum N\pi E^{5/4} K_{IC}^{-1} H_V^{-2} P^{7/4} \tag{4}$$

where K is a constant. Under identical conditions in ultrasonic machining:

$$\frac{V(\theta = 0^\circ)}{V(\theta = 90^\circ)} = \frac{K_{IC}^b}{K_{IC}^a} \tag{5}$$

As can be seen from Eq. (4) the volume loss fits the functional dependency of the $K_{IC}{}^{-1}$. Therefore, under identical conditions the highest MRR of specimen A in USM corresponded to its lowest value of fracture toughness. The ratio of $V(\theta=0^\circ)/\ V(\theta=90^\circ)$ equals that of $K_{IC}^b/\ K_{IC}^a$ [Eq. (5)]. It can be seen from Table 3 that the test results of the ratio $\mathrm{MRR}(\theta=0^\circ)/\ \mathrm{MRR}(\theta=90^\circ)$ agree well with the ratio $K_{IC}^b/\ K_{IC}^a$ as listed in Table 2.

Fig. 6 illustrates schematically the interactions between the lateral crack caused by impact abrasive particles and the whiskers, which occurred in each case respectively. For $\theta=0^\circ$, most of the whiskers were distributed parallel to the machining surface, and the lateral crack caused by the impact particles propagated in the direction parallel to the whisker plane (Fig. 6a). The

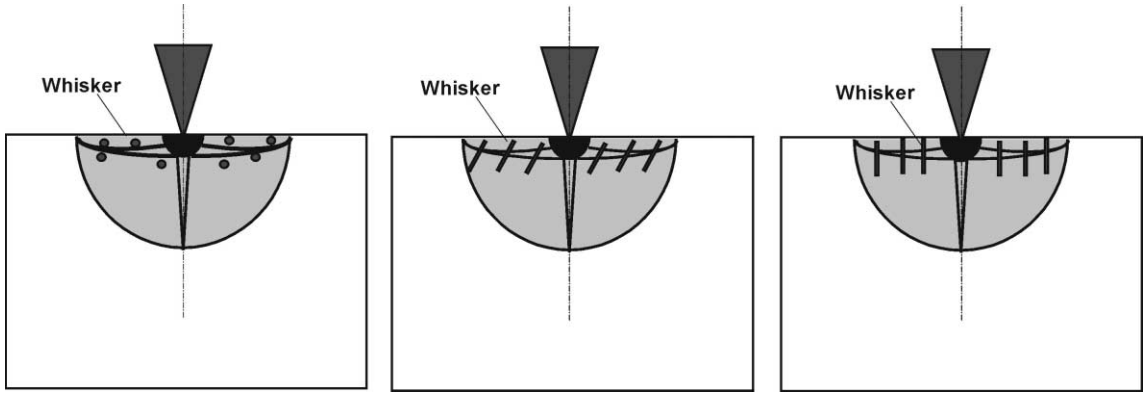

Fig. 6. Schematic illustration of the interactions between the abrasive particles and the whiskers of specimens when (a) $\theta=0^\circ$, (b) $\theta=45^\circ$ and (c) $\theta=90^\circ$ surface are used as machining surface.

whiskers no longer shared the load, and bridging rarely occurred. Little or no whisker toughening took place since lateral crack could readily propagate through the matrix. Hence, it can be stated that for this type of machining, the whiskers remain unfractured during USM, and they cannot support any applied stresses and act as effective toughening elements. The material removal was thought to occur primarily by surface chipping when lateral cracks curved up and intersected the surface. So in this case, larger MRR was observed in USM of the composites. SEM micrographs of the ultrasonic machined surfaces with $\theta = 0^\circ$ are shown in Fig. 7. It can be seen from the micrographs that a lot of whisker-like deep microgrooves and unfractured whiskers existed on the machined surface of the composite. These whisker-like deep microgrooves and unfractured whiskers indicated whisker debonding, which provided sufficient evidence that little or no whisker pullout and bridging took place during this type of USM.

Changes in the direction angle of the inclined whisker plane to the crack propagation direction influenced the contributions to toughening from bridging, pullout and crack deflection. When the direction angle θ between the whisker plane and the lateral crack propagation direction was changed from $\theta = 0$ to $\theta = 90^\circ$, for example $\theta = 45^\circ$ (Fig. 6b), the crack propagation direction was not normal to the whisker plane. In this case, the whiskers experienced both tensile and bending stresses, and there was an increased probability of whisker fracture along the line of matrix cracking because of the bending force on the whiskers. SEM micrographs of the ultrasonic machined surfaces with $\theta = 45^\circ$ are presented in Fig. 8.

While for $\theta = 90^\circ$ surface most of the whiskers were distributed normal to the machining surface, the lateral crack caused by the impact particles propagated in the direction perpendicular to the whisker axis (Fig. 6c), and the whisker experienced tensile stresses. The bridging whiskers imposed closure stress at the crack tip, acted as the major load-bearing element and resisted to crack propagation. Thus in the case of $\theta = 90^\circ$, the whiskers could be loaded to a greater extent than for the other cases, the resistance to whisker pullout dissipated energy and was, therefore, the main cause of the lowest MRR in USM of the composites. The SEM micrographs of the machined surface with $\theta = 0^\circ$ are reported in Fig. 9. When compared with Figs. 7 and 8, there were few microgrooves and unfractured whiskers on the machined surface. This substantiates the occurrence of whisker pullout and bridging. The whiskers have been pulled out from the matrix from one crack face in the wake of the crack tip, leaving protruding whiskers and associated holes on the machined surface, which provides sufficient evidence for the effect of whisker reinforcement during this type of USM.

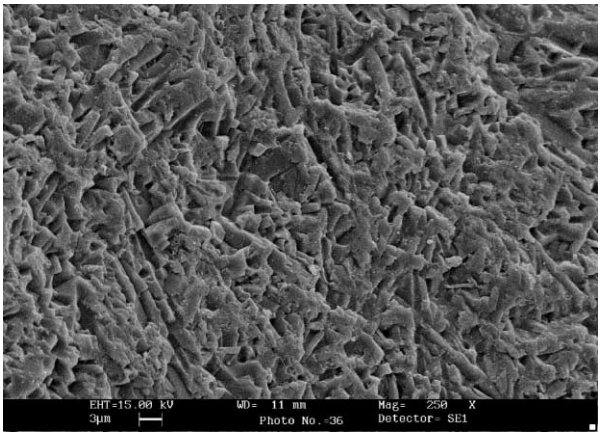

Fig. 7. SEM micrograph of the ultrasonic machined surfaces with $\theta = 0^\circ$ for Al_2O_3/SiC_w composites with 30 vol.% whiskers.

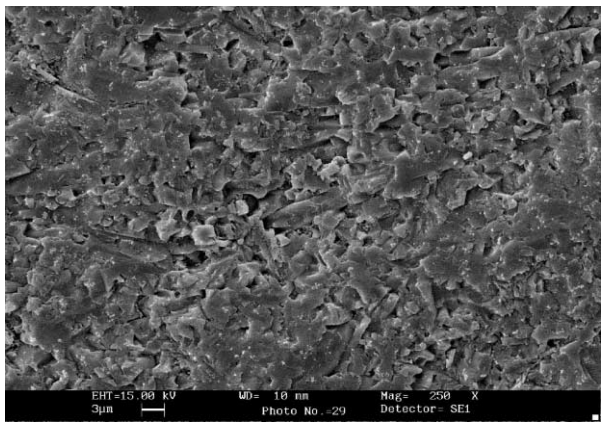

Fig. 8. SEM micrograph of the ultrasonic machined surfaces with $\theta = 45^\circ$ for Al_2O_3/SiC_w composites with 30 vol.% whiskers.

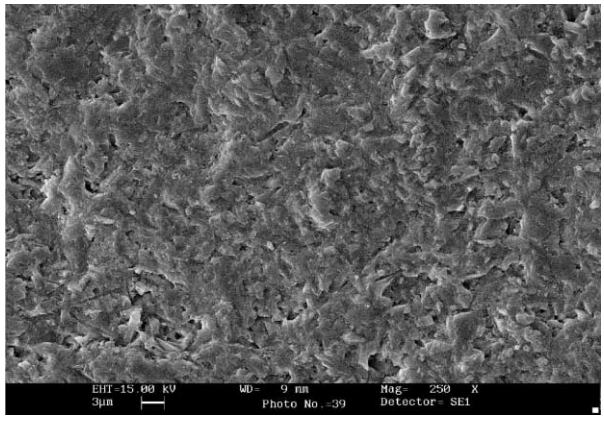

Fig. 9. SEM micrograph of the ultrasonic machined surfaces with $\theta = 90^\circ$ for Al_2O_3/SiC_w composites with 30 vol.% whiskers.

5. Conclusions

Effect of whisker orientation on the material removal rate and mechanisms in ultrasonic machining of SiC whisker-reinforced alumina ceramic composites have been studied. The following conclusions were obtained:

1. In ultrasonic machining of Al_2O_3/SiC_w ceramic composites, the material removal rate depends strongly on whisker orientation. The MRR vary on surfaces with different direction angle θ normal to the hot pressing direction. The maximum MRR is observed when the $\theta = 0^\circ$ surface is used as the machining surface, and the minimum values is observed at $\theta = 90^\circ$. This effect was even greater for the specimen with higher SiC whisker content.
2. The effect of whisker orientation on the machined surface roughness exhibits a similar outline than for MRR. The specimen with higher SiC whisker content shows the lowest surface roughness among the specimens tested.
3. The anisotropy of material removal rates and mechanisms with the direction angle in ultrasonic machining of the composites can be explained by the lateral crack fracture model. For $\theta = 0^\circ$, little or no whisker toughening takes place since the whiskers share no load, and lateral crack could readily propagate through the matrix. On the contrary for $\theta = 90^\circ$ surface the bridging whiskers impose closure stress at the crack tip and resist to crack propagation.

Acknowledgements

The work described in this paper has been supported by the Research Grants Council of Hong Kong, China (PolyU 5173/97E).

References

[1] A.G. Evans, Perspective on the development of high toughness ceramics, J. Am. Ceram. Soc. 73 (2) (1990) 187–206.
[2] P.F. Becher, Microstructural design of toughened ceramics, J. Am. Ceram. Soc. 74 (2) (1991) 255–269.
[3] P.F. Becher, G.C. Wei, Toughening behavior in SiC-whisker reinforced alumina, J. Am. Ceram. Soc. 67 (12) (1984) 267–269.
[4] T.N. Tiegs, P.F. Becher, Sintered Al_2O_3/SiC whisker composites, Am. Ceram. Soc. Bull. 66 (1987) 339–442.
[5] H.K. Tönshoff, H. Trumpold, Evaluation of surface layers of machined ceramics, Annals of the CIRP 38 (2) (1989) 699–708.
[6] N.F. Petrofes, Shaping ceramic with electrical discharge machining, PhD dissertation, Texas A&M University, 1989.
[7] F. Lee, M.S. Sandlin, Toughness anisotropy in textured ceramics, J. Am. Ceram. Soc. 76 (6) (1993) 1793–1800.
[8] J. Vigneau, P. Bordel, Influence of the microstructure of the composite ceramic tools on their performance when machining nickel alloys, Annals of the CIRP 36 (1987) 13–16.
[9] D. Jianxin, A. Xing, Effect of whisker orientation on the friction and wear behavior of $Al_2O_3/TiB_2/SiC_w$ composites in sliding wear tests and in machining processes, Wear 201 (1996) 178–185.
[10] B.R. Lawn, A.G. Evans, D.B. Marshall, Elastic/plastic indentation damage in ceramics: the median/radial crack system, J. Am. Ceram. Soc. 63 (9–10) (1980) 574–581.
[11] D.B. Marshall, B.R. Lawn, A.G. Evans, Elastic/plastic indentation damage in ceramics: the lateral crack system, J. Am. Ceram. Soc. 65 (11) (1982) 561–566.
[12] H. Kamiya, M. Sakakibara, Y. Sakurai, Erosion wear properties of tetragonal ZrO_2 (Y_2O_3)-toughened Al_2O_3 composites, J. Am. Ceram. Soc. 77 (3) (1994) 666–672.